Journal of Power Sources 231 (2013) 213–218

Contents lists available at SciVerse ScienceDirect

Journal of Power Sources

journal homepage: www.elsevier.com/locate/jpowsour

Short communication

Preparation and evaluation of $BaZr_{0.1}Ce_{0.7}Y_{0.1}Yb_{0.1}O_{3-\delta}$ (BZCYYb) electrolyte and BZCYYb-based solid oxide fuel cells

Ngoc Thi Quynh Nguyen, Hyon Hee Yoon*

Dept. of Chemical and Bio Engineering, Gachon University, Seongnam, Gyeonggi-Do 461-701, Republic of Korea

HIGHLIGHTS

- ► Crystalline powders of BZCYYb with a high sintering activity were prepared by coprecipitation.
- ► The BZCYYb sample sintered at 1500 °C for 5 h exhibited a relative density of 98%.
- ► The ionic conductivities of the BZCYYb were 7.4×10^{-2} S cm^{-1} at 750 °C and 1.9×10^{-2} S cm^{-1} at 500 °C.
- ► An anode-supported cell based on the BZCYYb exhibited a maximum power density of 1.0 W cm^{-2} at 750 °C.

ARTICLE INFO

Article history:
Received 7 November 2012
Received in revised form
21 December 2012
Accepted 1 January 2013
Available online 9 January 2013

Keywords:
Solid oxide fuel cell
Proton conductor
Doped barium cerate
Carbonate coprecipitation
Spin coating

ABSTRACT

$BaZr_{0.1}Ce_{0.7}Y_{0.1}Yb_{0.1}O_{3-\delta}$ (BZCYYb) electrolyte powders are prepared by ammonium carbonate coprecipitation. Crystalline fine powders with a pure perovskite phase are obtained by the calcination of the precursor powders at 1000 °C. The relative densities of the sample pellets sintered at 1400 and 1500 °C for 5 h are 96.5 and 97.9% (% of theoretical), respectively. The electrical conductivities of the BZCYYb electrolytes exhibit high values of 1.9×10^{-2} S cm^{-1} at 500 °C and 7.4×10^{-2} S cm^{-1} at 750 °C with an activation energy of 0.45 eV. An anode-supported cell is also fabricated from the synthesized BZCYYb electrolyte using spin coating. A dense, crack-free 10-μm-thick electrolyte film has been successfully fabricated. The fabricated single cell exhibits promising performance, with maximum power densities of 1.0 W cm^{-2} at 750 °C and 0.23 W cm^{-2} at 500 °C.

1. Introduction

Solid oxide fuel cells (SOFCs) have received significant attention as alternative electric power generation systems because of their high energy conversion efficiency (up to 60%), fuel flexibility, and low pollutant emission [1–3]. The typical operating temperature of stabilized zirconia (YSZ)-based SOFCs is near 1000 °C. The high operating temperature of SOFCs makes the manufacturing processes expensive and results in long-term reliability problems. The operating temperature of SOFCs depends mainly on the electrolyte material of the SOFC because ionic charge transport is far more difficult than electron charge transport. Therefore, the development of new electrolyte materials with high ionic conductivities is a major challenge in the development of low-temperature SOFCs. A variety of oxide ion conducting materials have recently been reported, including gadolinium-doped ceria (GDC), samarium-doped ceria (SDC), bismuth yttrium oxide (BYO), and strontium- and magnesium-doped lanthanum gallate (LSGM) [4,5].

After the high proton conductivities of cerates were first reported in the1980's [6,7], proton conducting materials have received tremendous attention as promising electrolytes for low-temperature SOFCs because of their advantages over oxide ion conducting electrolytes, including their higher ionic conductivity at lower temperatures (500–700 °C) than the typical SOFC operating temperatures and a lack of fuel dilution in the anode due to water formation at the cathode side [8–11]. Currently, $BaCeO_3$ and $BaZrO_3$ are state-of-the-art proton-conducting materials. These perovskite-type oxides have been doped with various divalent or trivalent cations, including Y, Yb, Gd, Sm, Nd, and La, to obtain materials with high conductivity and sufficient chemical and thermal stability over a range of SOFC operating conditions [9,12–14]. The doped $BaCeO_3$ has high proton conductivity but poor chemical stability. In contrast, $BaZrO_3$ has relatively low conductivity but good chemical stability. Hence, solid solutions of doped $BaCeO_3$ and $BaZrO_3$, such as $BaZr_{0.1}Ce_{0.7}Y_{0.2}O_{3-\delta}$ (BZCY),

* Corresponding author. Tel.: +82 31 750 5356; fax: +82 31 750 5363.
E-mail address: hhyoon@gachon.ac.kr (H.H. Yoon).

0378-7753/$ – see front matter © 2013 Elsevier B.V. All rights reserved.
http://dx.doi.org/10.1016/j.jpowsour.2013.01.011

have been widely investigated to achieve both good chemical stability and proton conductivity [15,16]. Further improvement of BZCY by codoping with Yb has also been reported [17,18]. Barium zirconate-cerate codoped with Y and Yb ions (BZCYYb) was reported to exhibit higher conductivity than BZCY as well as the conventional oxide ion conductors such as YSZ and GDC at low operating temperatures (400–750 °C) [17]. The BZCYYb electrolyte can facilitate the transport of both proton and oxide ion vacancies depending on the fuel cell operating conditions and has highly desirable properties, especially for use in hydrocarbon-fueled-SOFCs, such as enhanced sulfur and coking tolerances [17].

The $BaCeO_3$- and $BaZrO_3$-based SOFC electrolyte materials have been prepared by conventional solid-state reaction [15,17], sol–gel [15,16], combustion [18–20], and coprecipitation [21–23] methods. Because high sintering temperatures (~1600 °C) are generally required for the densification of $BaCeO_3$ and $BaZrO_3$, lowering the sintering temperature substantially reduces the fabrication cost and prevents the possible formation of a secondary phase at the electrolyte/electrode interfaces. In this context, coprecipitation is a promising method for the preparation of fine metal oxide precursor powders that can be sintered at low temperatures [24]. It is a relatively simple and economic process, and is conventionally used in the production of supported catalysts. The preparation of barium cerate doped with Nd [21] and Ca ion [22] via an oxalate precursor has been reported. The synthesis of BZCY via a carbonate precursor has also been reported [23]. The sintered BZCY exhibited a low grain boundary resistance due to the fine crystalline green powder with excellent stoichiometry [23].

In this study, $BaZr_{0.1}Ce_{0.7}Y_{0.1}Yb_{0.1}O_{3-\delta}$ (BZCYYb) was prepared by carbonate precipitation and a single cell was fabricated using BZCYYb electrolyte film by spin coating. The ionic conductivity and cell performance were then investigated. The primary objective of this work was to prepare BZCYYb powders with high sintering ability and high ionic conductivity and to fabricate an anode-supported single cell with a high power density using the synthesized BZCYYb powders.

2. Experimental

2.1. Powder preparation

$BaZr_{0.1}Ce_{0.7}Y_{0.1}Yb_{0.1}O_{3-\delta}$ (BZCYYb) electrolyte powders were synthesized using the ammonium carbonate ($(NH_4)_2CO_3$) coprecipitation method. $Ba(NO_3)_2$, $Zr(NO_3)_2{\cdot}6H_2O$, $Ce(NO_3)_3{\cdot}6H_2O$, $Y(NO_3)_3{\cdot}6H_2O$, and $Yb(NO_3)_3{\cdot}6H_2O$, were used as the starting salts. Stoichiometric amounts of each component (corresponding to the $BaZr_{0.1}Ce_{0.7}Y_{0.1}Yb_{0.1}O_{3-\delta}$ final product) were dissolved in deionized-water to obtain a metal ion solution with a total metal ion concentration of 0.5 M. The precursor metal solution was then dropped into a 5% ammonium carbonate solution under gentle stirring. The solution containing the precipitates was incubated with stirring at 400 rpm at 60 °C for 3 h. The precipitate was then filtered off, washed, and dried. The dried precursor powder was ground in a mortar and then calcined at different temperatures (900, 1000, and 1100 °C). The calcined powder was used as the electrolyte powder in the preparation of a single cell. This powder was also pelletized into a disk shape through compression at 80 MPa. The pellets were sintered at various temperatures for 5 h in air and used for the conductivity measurements.

2.2. Fabrication of an anode-supported single cell

The BZCYYb powder was mixed with NiO nanopowder (<50 nm, Aldrich) at a weight ratio of 35:65. The mixture was then ball-milled in ethanol for 24 h. Next, the suspension was dried to evaporate the ethanol. The obtained powder was ground and sieved. The final powder is referred to as the anode powder. To prepare the electrolyte slurry for spin coating, the BZCYYb powder was mixed with an organic vehicle (3% ethyl cellulose and 97% terpinol). The cathode slurry was prepared by mixing BZCY powder and lanthanum strontium cobaltite ferrite (LSCF) at a 3:7 weight ratio with an aliquot of an organic vehicle (6% ethyl cellulose and 94% terpinol). First, the anode powder was pressed into disks of 31 mm diameter at 26 MPa, followed by pre-firing at 800 °C for 2 h to form an anode substrate. The BZCYYb slurry was spin-coated onto the NiO–BZCYYb anode substrate and then sintered at 1400 °C for 5 h. The BZCY–LSCF slurry was screen-printed onto the top of the BZCYYb electrolyte layer, which was then fired at 1000 °C for 2 h. The thicknesses of the electrolyte and cathode were approximately 10 and 20 μm, respectively. The effective area of the cathode was 0.75 cm^2.

2.3. Characterization

The crystalline structures of the BZCYYb powder and sintered pellets were analyzed by X-ray diffractometry (XRD; Rigaku D/MAX-2200) with Cu Kα radiation at a wavelength of 1.5406 Å. XRD was performed at 40 kV and 20 mA in the range of $2\theta = 20$–90° with a scanning speed of 4 θ min^{-1}. Powder size was determined by a laser scattering particle size analyzer (Brookhanven/BI-9000AT). Field emission scanning electron microscopy (SEM; Hitachi S-4700) was used to characterize the morphology of the BZCYYb powder, the sintered pellets, and the single cell. The density of sintered the BZCYYb pellet was determined based on geometrical measurements and a water immersion (Archimedes) method. The ionic conductivity and cell performance were measured as a function of temperature from 500 to 750 °C using a two-probe AC impedance analyzer (Solartron 1280B) with a frequency range of 0.1 Hz–1.0 MHz with a signal amplitude of 10 mV. For the ionic conductivity analysis, both faces of the sintered BZCYYb pellets were coated with platinum paste, followed by firing at 900 °C for 1 h. In the cell performance test, the anode side was exposed to humidified hydrogen (~3% vol H_2O) with a flow rate of 100 ml min^{-1} and the cathode was exposed to ambient air. Pt paste was applied to the cathode as a current collector and Pt wire was used as the conducting wire. The cell current and voltage characteristics were evaluated in the temperature range of 500–750 °C.

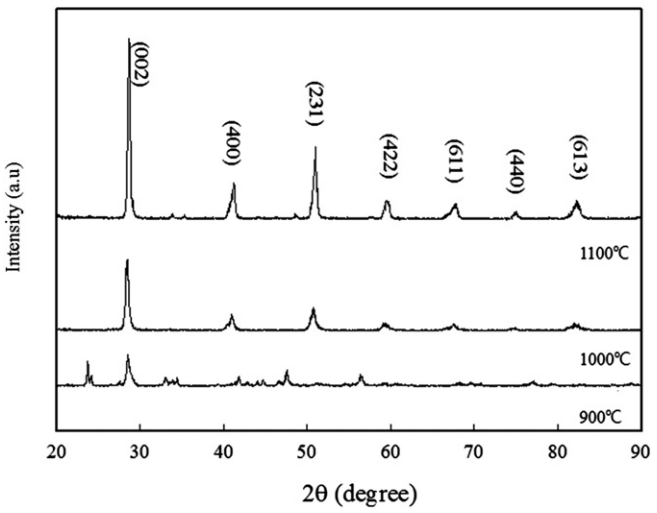

Fig. 1. XRD patterns of BZCYYb powders calcined at different temperatures (900 °C, 1000 °C, 1100 °C).

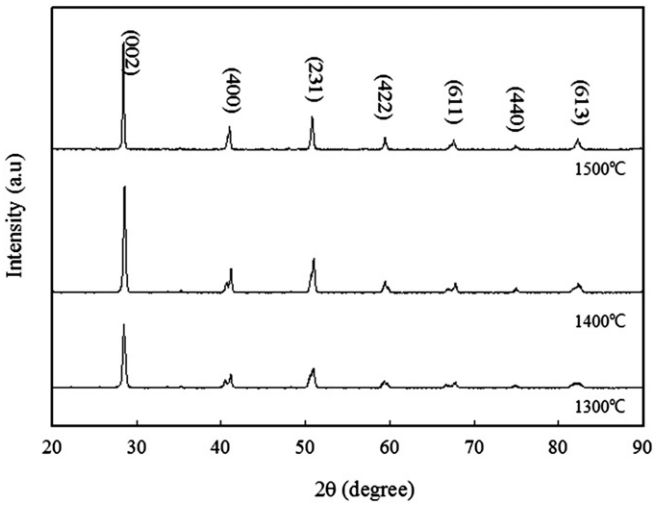

Fig. 2. XRD patterns of BZCYYb pellets sintered at different temperatures (1300 °C, 1400 °C, 1500 °C).

3. Results and discussion

3.1. Structural and morphological properties

The XRD patterns of the BZCYYb powder calcined at different temperatures are presented in Fig. 1. The BZCYYb powders calcined at 900 °C exhibited a perovskite structure with secondary phases. When the calcination temperature was at or above 1000 °C, a pure perovskite phase was observed. The observed peaks in the XRD pattern of powder calcined at 1000 °C or above were indexed to the orthorhombic structure of perovskite-type $BaCeO_3$. Fig. 2 shows the XRD patterns of the BZCYYb pellets sintered at different temperatures. The XRD patterns for the sintered pellets were similar to those of the powders; however, the peak intensity was considerably higher for the pellets. As the sintering temperature increased in the range of 1300–1500 °C, the peak intensity also increased.

The SEM images of calcined BZCYYb powders and sintered BZCYYb pellets are shown in Fig. 3. The calcined powders at 1000 °C were finely divided and a typical size of powder grain ranged from 50 to 150 nm, as determined from the SEM images (Fig. 3(a) and (b)). The apparent particle size growth was observed at the higher calcination temperature of 1100 °C (Fig. 3(a) and (c)). The particle

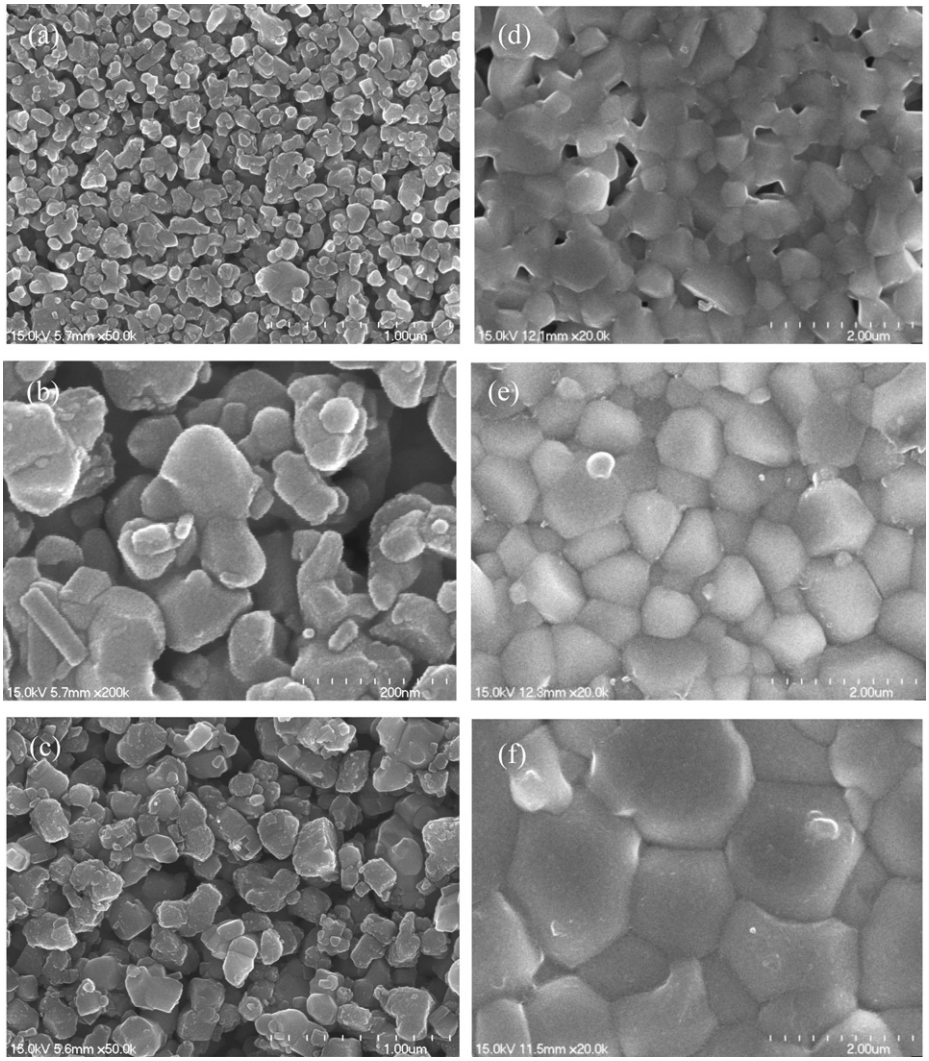

Fig. 3. SEM morphologies of the BZCYYb powders calcined at 1000 °C (at low (a) and high (b) magnification) and 1100 °C (c) and of the BZCYYb pellets sintered at 1300 °C (d), 1400 °C (e), and 1500 °C (f).

sizes of BZCYYb powders calcined at 1000 and 1100 °C were in the range of 140–180 nm, and 210–360 nm, respectively, as determined by laser scattering. The sintering behavior also varied with the calcination temperature; after sintering at 1400 °C for 5 h, the relative densities of the BZCYYb pellets from powders calcined at 1000 and 1100 °C were measured to be 96.5, and 90.1%, respectively. This result indicates that BZCYYb powders calcined at 1000 °C exhibited higher sintering activity than those calcined at 1100 °C due to the smaller particle size. It should be noted that the dilatometry test was failed because the BZCYYb sample reacted with the alumina sample holder forming a liquid phase. A well-sintered surface without residual pores was observed for the BZCYYb samples sintered at 1400 and 1500 °C. The grain size of the BZCYYb pellet increased with an increase in the sintering temperature. A typical grain size of the BZCYYb pellets was in the range of 1–3 μm. The relative densities (% of theoretical) of the sintered pellets were also measured. The theoretical density of BZCYYb was calculated from the lattice parameters of the BZCYYb sample calcined at 1000 °C. As shown in Fig. 3(b), the BZCYYb pellet sintered at 1300 °C for 5 h contained a significant number of pores; thus the relative density was as low as 74.1%. On the other hand, the BZCYYb pellets sintered at 1400 and 1500 °C for 5 h were quite dense (96.5% and 97.9%, respectively) and lacked visible pores, as shown in Fig. 3(e) and (f). These results are comparable with the values reported previously; the BZCYYb powder prepared by glycine nitrate-combustion was sintered at 1400 °C for 10 h to achieve a density of 98.4% [18].

3.2. Electrical conductivity

The electrical conductivity of the BZCYYb electrolyte was measured using an AC impedance analyzer at temperatures ranging from 500 to 750 °C. The impedance spectra of the pellet sintered at 1500 °C are shown in Fig. 4. The axis intercept and the semicircle were attributed to the bulk resistance and grain boundary resistance, respectively. The bulk and grain boundary conductivities of the BZCYYb samples were calculated from the resistance data and are presented in Fig. 5. The BZCYYb samples sintered at 1400 and 1500 °C exhibited almost the same bulk conductivity (Fig. 5(a)); however, a higher grain boundary conductivity was observed at the higher sintering temperature (Fig. 5(b)) because the BZCYYb samples sintered at higher temperatures contained larger grains, as observed in the SEM images in Fig. 3. At 500 and 750 °C, the grain boundary resistances were approximately 30% and 25% of the bulk resistance, respectively. The low grain boundary resistances might indicate that the formation of the secondary phase and/or the accumulation of impurities at the grain boundaries during sintering and grain growth were reduced by the use of a pure starting oxide powder prepared by ammonium carbonate precipitation. A similar result was previously obtained for BZCY electrolytes [23]. The highest total conductivities (1.9×10^{-2} S cm^{-1} at 500 °C and

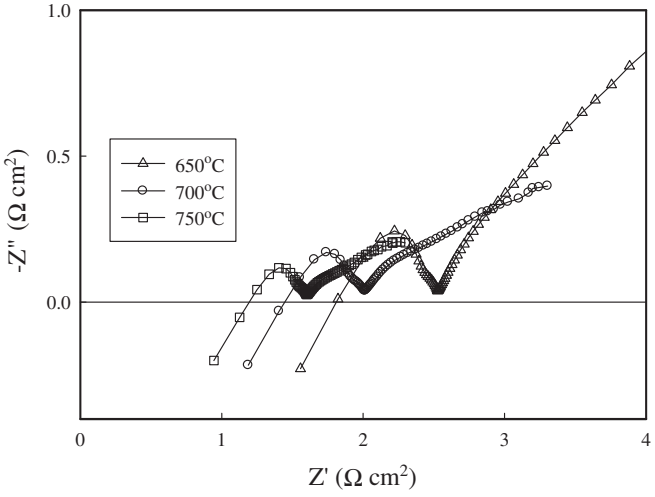

Fig. 4. Impedance spectra of the BZCYYb pellet sintered at 1500 °C measured at different temperatures in wet air.

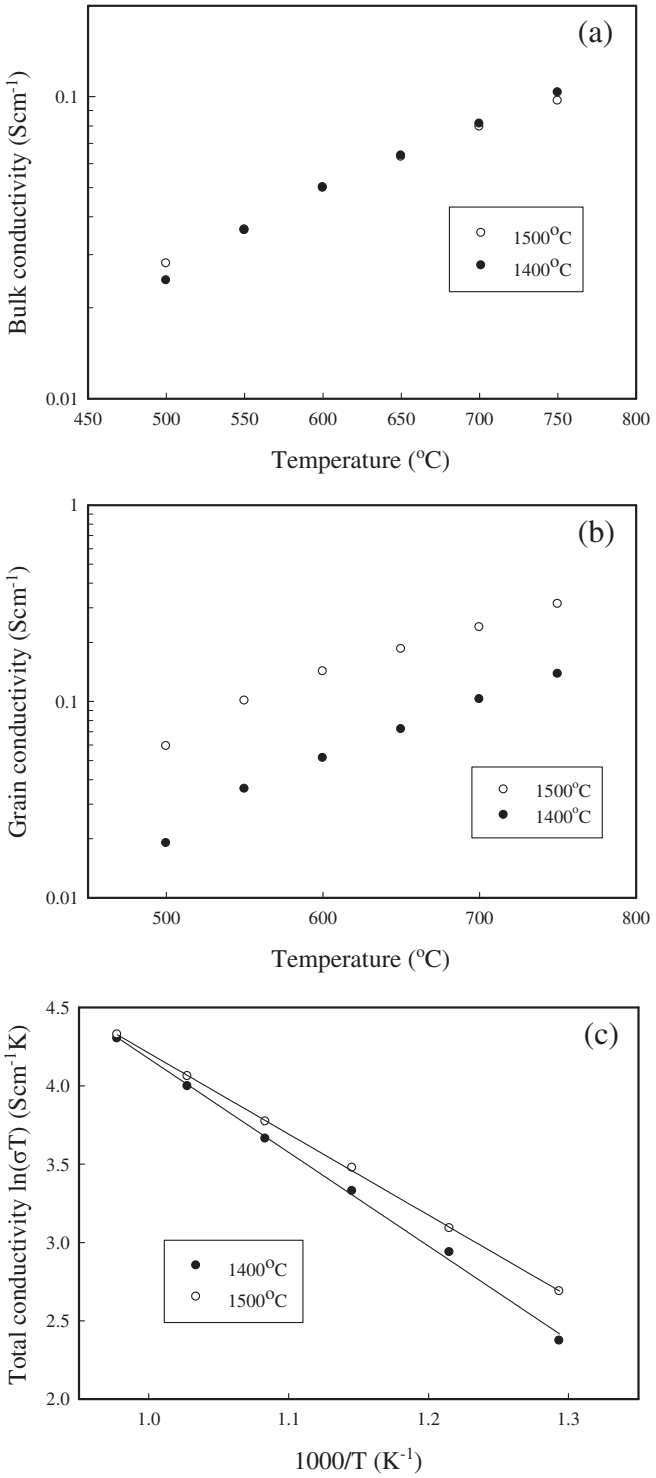

Fig. 5. Bulk (a) and grain boundary (b) conductivities and Arrhenius plot of total conductivity (c) of BZCYYb pellets sintered at different temperatures.

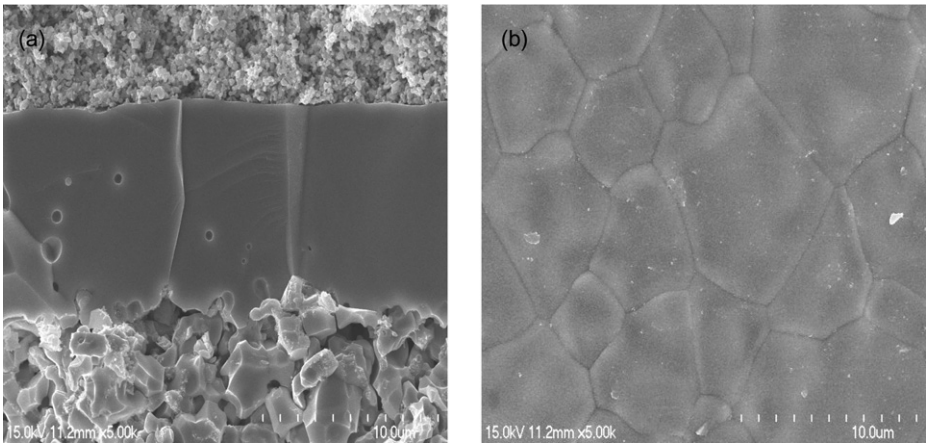

Fig. 6. SEM images of the cross-section of the single cell (Ni–BZCYYb|BZCYYb|BZCYYb–LSCF) (a) and the surface of BZCYYb electrolyte film (b).

7.4×10^{-2} S cm^{-1} at 750 °C) with a conduction activation energy of 0.45 eV were observed for the BZCYYb pellet sintered at 1500 °C. These electrical conductivity values are comparable to those reported in previous studies [17,18]. These results indicate that the ammonium carbonate coprecipitation method could be used in the preparation of BZCYYb electrolytes for practical SOFC applications.

3.3. *I–V* and power density

The cross-sectional SEM image of the anode-supported single cell (Ni-BZCYYb|BZCYYb|BZCYYb–LSCF) is presented in Fig. 6. The electrolyte film was prepared by slurry spin-coating. It was approximately 10 μm thick and adhered well to the anode support. No connecting pores were observed in the electrolyte thin films. The high-density and crack-free properties of the electrolyte film were also confirmed by measuring the open circuit voltage (OCV). Fig. 7 shows the OCVs of the single cell from 500 to 750 °C with humidified H_2 as the fuel and ambient air as the oxidant. The Nernst potentials were included in Fig. 7 for comparison. The recorded OCVs were slightly lower than the theoretical values; the deviations from Nernst potential were 0.04 V at 500 °C and 0.2 V at 750 °C, probably due to the electron conduction through the electrolyte layer and/or imperfect seals between the electrodes. Electronic conduction in the ceria-based thin electrolyte layer under reduction conditions has been reported to be unavoidable because of the partial reduction of Ce^{4+} into Ce^{3+} at low oxygen partial pressure [28,29]. The lower OCV will eventually decrease the power density [19]. The OCV values of the 10-μm-thick BZCYYb-based cell were, however, close to the theoretical values (1.12 V at 500 °C and 0.94 V at 750 °C), suggesting that the electron conduction through the BZCYYb electrolyte layer were insignificant. A similar result was reported previously [17]. The *I–V* and power density curves of the anode-supported single cell are shown in Fig. 8. The maximum power densities were 1.0 W cm^{-2} at 750 °C and 0.23 W cm^{-2} at 500 °C. The cell performance obtained in this work is close to the highest values reported for BZCYYb electrolyte-based SOFCs (1.1 W cm^{-2} at 750 °C [17], 1.13 W cm^{-2} at 750 °C [25], 0.49 W cm^{-2} at 700 °C [26]).

The impedance spectra and the estimated resistances of a single cell measured under open-circuit conditions at different temperatures are shown in Fig. 9. The ohmic resistance (R_o), which is mainly due to the electrolyte, was determined from the high-frequency intercept with the real axis. The polarization resistance of the electrodes (R_p), which is mainly caused by the electrochemical activity and the microstructure of the electrodes and interfaces, was determined from the difference between the high- and low-frequency intercepts with the real axis. The total cell resistance

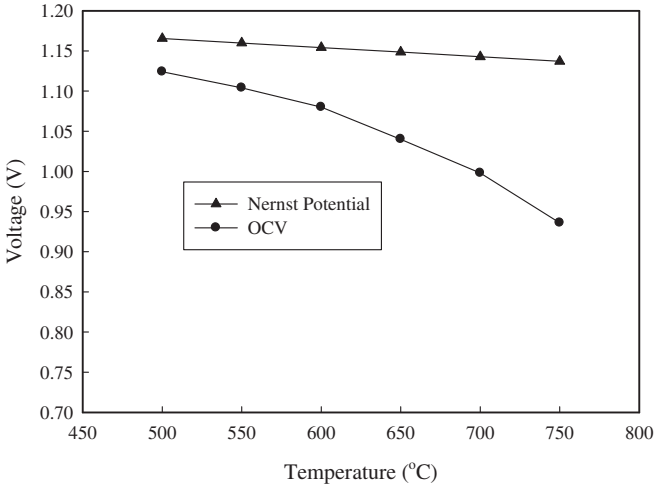

Fig. 7. Open circuit voltages (OCVs) of the Ni–BZCYYb|BZCYYb|BZCY–LSCF cell at different operating temperatures with humidified H_2 as the fuel and ambient air as the oxidant.

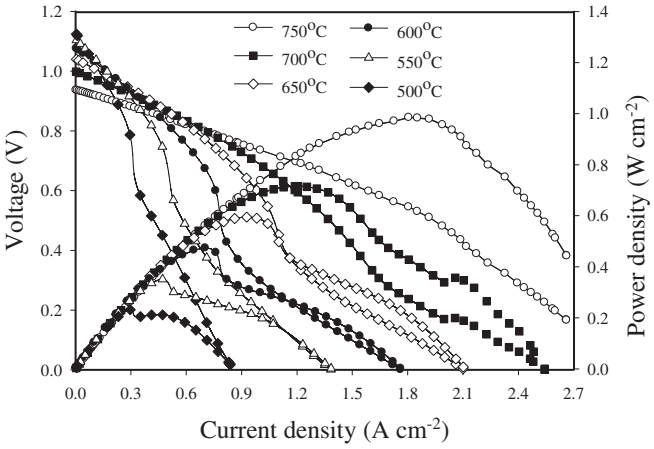

Fig. 8. The *I–V* and power density curves of the Ni–BZCYYb|BZCYYb|BZCY–LSCF cell at different operating temperatures with humidified H_2 as the fuel and ambient air as the oxidant.

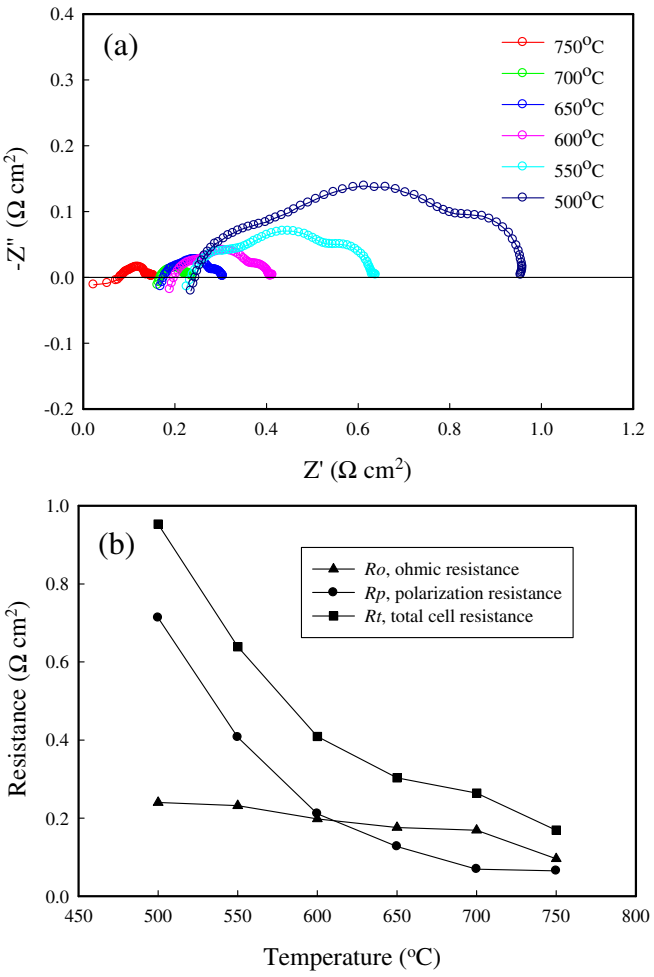

Fig. 9. Impedance spectra (a) of the Ni–BZCYYb|BZCYYb|BZCY–LSCF cell measured at different temperatures under open-circuit conditions, and (b) the total cell resistance (R_t), interfacial polarization resistance (R_p), and ohmic resistance (R_o) as determined from the impedance spectra as shown in (a).

(R_t) is the sum of R_o and R_p, corresponding to the intercept with the real axis at low frequencies [27]. As shown in Fig. 9, the polarization resistance increased significantly as the cell operating temperature decreased, whereas the ohmic resistance was less dependent on the temperature. This result suggests that electrodes with better catalytic performance and optimized microstructure are needed to reduce the electrode polarization resistance and thus improve the cell performance, especially at low operating temperatures.

4. Conclusions

The present study demonstrates that fine crystalline BZCYYb electrolyte powders with a high sintering activity can be successfully synthesized by the coprecipitation method using ammonium carbonate as a precipitant. Fine crystalline powders with pure perovskite phase and a high sintering activity are obtained by the calcination of the precursor powders at 1000 °C. Relative densities of 96.5 and 97.9 (% of theoretical) are obtained after sintering the calcined powders at 1400 and 1500 °C for 5 h, respectively. The electrical conductivities of BZCYYb are 1.9×10^{-2} S cm^{-1} at 500 °C and 7.4×10^{-2} S cm^{-1} at 750 °C with an activation energy of 0.45 eV. An anode-supported cell is also fabricated using the synthesized BZCYYb electrolyte via a spin-coating method. A dense, crack-free 10-μm-thick electrolyte film is successfully fabricated. The fabricated single cell exhibits promising performance, with maximum power densities of 1.0 W cm^{-2} at 750 °C and 0.23 W cm^{-2} at 500 °C. The results of this study indicate that BZCYYb electrolytes have excellent properties for use in low-temperature-SOFCs and that the simple and cost-effective ammonium carbonate coprecipitation method is a practical method for the preparation of BZCYYb electrolytes.

Acknowledgments

This research was supported by the Basic Science Research Program through the National Research Foundation of Korea (NRF) funded by the Ministry of Education, Science and Technology (2010-0022930).

References

[1] N.Q. Minh, T. Takahashi, Science and Technology of Ceramic Fuel Cells, Elsevier, Amsterdam, 1995.
[2] A.J. Jacobson, Chem. Mater. 22 (2010) 660.
[3] K. Sasaki, K. Watanabe, K. Shiosaki, K. Susuki, Y. Teraoka, J. Electroceram. 13 (2004) 669.
[4] S. Hui, J. Roller, S. Yick, X. Zhang, C. Decès-Petit, Y. Xie, R. Maric, D. Ghosh, J. Power Sources 172 (2007) 493.
[5] D.J.L. Brett, A. Atkinson, N.P. Brandon, S.J. Skinner, Chem. Soc. Rev. 37 (2008) 1568.
[6] H. Iwahara, T. Esaka, H. Uchida, N. Maeda, Solid State Ionics 3–4 (1981) 359.
[7] H. Iwahara, H. Uchida, K. Kondo, K. Ogaki, J. Electrochem. Soc. 135 (1988) 529.
[8] K.D. Kreuer, Chem. Mater. 8 (1996) 610.
[9] F. Lefebvre-Joud, G. Gauthier, J. Mougin, J. Appl. Electrochem. 39 (2009) 535.
[10] A.K. Demin, P.E. Tsiakaras, V.A. Sobyanin, S.Yu. Hramova, Solid State Ionics 152–153 (2002) 555.
[11] G. Meng, G. Ma, Q. Ma, R. Peng, X. Liu, Solid State Ionics 178 (2007) 697.
[12] D.A. Stevenson, N. Jiang, R.M. Buchanan, F.E.G. Henn, Solid State Ionics 62 (1993) 279.
[13] H. Iwahara, T. Yajima, H. Ushida, Solid State Ionics 70/71 (1994) 267.
[14] M. Oishi, K. Yashiro, K. Sato, J. Mizusaki, N. Kitamura, K. Amezawa, T. Kawada, Y. Uchimoto, Solid State Ionics 179 (2008) 529.
[15] P. Sawant, S. Varma, B.N. Wani, S.R. Bharadwaj, Int. J. Hydrogen Energy 37 (2012) 3848.
[16] Y. Guo, Y. Lin, R. Ran, Z. Shao, J. Power Sources 193 (2009) 400.
[17] L. Yang, S.Z. Wang, K. Blinn, M.F. Liu, Z. Liu, Z. Cheng, M.L. Liu, Science 326 (2009) 126.
[18] X.L. Zhou, L.M. Liu, J.M. Zhen, S.C. Zhu, B.W. Li, K.N. Sunand, P. Wang, J. Power Sources 196 (2011) 5000.
[19] W. Sun, Y. Wang, S. Fang, Z. Zhu, L. Yan, W. Liu, Electrochim. Acta 56 (2011) 1447.
[20] C.L. Tsai, M. Kopczyk, R.J. Smith, V.H. Schmidt, Solid State Ionics 181 (2010) 1083.
[21] S.D. Flint, R.C.T. Slade, Solid State Ionics 77 (1995) 215.
[22] F. Chen, P. Wang, O.T. Sørensen, G. Meng, D. Peng, J. Mater. Chem. 7 (1997) 1533.
[23] Zhimin Zhong, Solid State Ionics 178 (2007) 213.
[24] J.G. Li, T. Ikegami, T. Mori, T. Wada, Chem. Mater. 13 (2001) 2913.
[25] C. Chen, M. Liu, Y. Bai, L. Yang, E. Xie, M. Liu, Electrochem. Commun. 13 (2011) 615.
[26] H. Ding, Y. Xie, X. Xue, J. Power Sources 196 (2011) 2602.
[27] Q.-A. Huang, R. Hui, B. Wang, J. Zhang, Electrochim. Acta 52 (2007) 8144.
[28] T. Yamaguchi, T. Suzuki, S. Shimizu, Y. Fujishiro, M. Awano, J. Membr. Sci. 300 (2007) 45.
[29] T. Matsui, M. Inaba, A. Mineshige, Z. Ogumi, Solid State Ionics 176 (2005) 647.